# Critical Regions for Assembly of Vertebrate Nonmuscle Myosin II†

Takashi Nakasawa,‡ Masayuki Takahashi,*,‡ Fumiko Matsuzawa,§ Seiichi Aikawa,§ Yuki Togashi,||,⊥ Takayuki Saitoh,||,@ Akihiko Yamagishi,||,▽ and Michio Yazawa‡

*Divisions of Chemistry and Biological Sciences, Graduate School of Science, Hokkaido University, Sapporo 060-0810, Japan, and Celestar Lexico-Sciences, Inc., Chiba 261-8501, Japan*

*Received June 8, 2004; Revised Manuscript Received October 22, 2004*

ABSTRACT: Myosin II molecules assemble and form filaments through their C-terminal rod region, and the dynamic filament assembly−disassembly process of nonmuscle myosin II molecules is important for cellular activities. To estimate the critical region for filament formation of vertebrate nonmuscle myosin II, we assessed the solubility of a series of truncated recombinant rod fragments of nonmuscle myosin IIB at various concentrations of NaCl. A C-terminal 248-residue rod fragment (Asp 1729−Glu 1976) was shown by its solubility behavior to retain native assembly features, and two regions within it were found to be necessary for assembly: 35 amino acid residues from Asp 1729 to Thr 1763 and 39 amino acid residues from Ala 1875 to Ala 1913, the latter containing a sequence similar to the assembly competence domain (ACD) of skeletal muscle myosin. Fragments lacking either of the two regions were soluble at any NaCl concentration. We referred to these two regions as nonmuscle myosin ACD1 (nACD1) and nACD2, respectively. In addition, we constructed an α-helical coiled-coil model of the rod fragment, and found that a remarkable negative charge cluster (termed N1) and a positive charge cluster (termed P2) were present within nACD1 and nACD2, respectively, besides another positive charge cluster (termed P1) in the amino-terminal vicinity of nACD2. From these results, we propose two major electrostatic interactions that are essential for filament formation of nonmuscle myosin II: the antiparallel interaction between P2 and N1 which is essential for the nucleation step and the parallel interaction between P1 and N1 which is important for the elongation step.

Myosins constitute a superfamily of actin-based molecular motors that are involved in cellular activities such as muscle contraction, organelle motility, cell migration, and cytokinesis (for reviews, see refs *1* and *2*). All types of myosins consist of a conserved N-terminal motor domain containing an actin-binding site and an ATP-binding site, a neck region that interacts with light chains and/or calmodulin, and a diverse C-terminal tail region. Myosin II, one of the best-studied members of the superfamily, is a hexamer composed of two heavy chains (MHCs) and two pairs of light chains with a molecular shape of two globular heads connected to long tails. Each head (the motor domain and the neck region) consists of the N-terminal region of the MHC and a pair of light chains, and the C-terminal regions of the two MHCs which form an α-helical coiled-coil structure constitute the rodlike tail. The tails are involved in the assembly of myosin II molecules into filaments. In the amino acid sequence of the tail region, the 28-amino acid repeating units containing four heptad repeats characteristic of coiled-coil proteins exhibit patches of negative and positive charges spaced 14 residues apart. These repeats were proposed to be responsible for the packing of the coiled-coil tails for formation of filaments through electrostatic interaction (*3*, *4*).

Among the two subclasses of vertebrate myosin II molecules, sarcomeric types from skeletal and cardiac muscle always form stable thick filaments under physiological conditions. On the other hand, the filament assembly−disassembly process appears to be dynamic *in vitro* in nonsarcomeric-type myosin II forms from smooth muscle and nonmuscle tissues (*1*, *5*). However, smooth muscle myosin II can form filaments even in the relaxed state *in vivo* (*6*, *7*). Dynamic assembly−disassembly transitions of myosin II molecules are important in nonmuscle cells, and are known to be organized spatiotemporally in response to certain signals, as demonstrated in studies of *Dictyostelium* myosin II (*8*, *9*). The understanding of the molecular mechanism for the filament assembly is advanced also in the studies of *Dictyostelium* (*10*−*12*) as well as of *Acanthamoeba* (*13*, *14*). It is noted, however, that these protozoan myosin II forms are classified in subclasses different from those of vertebrate nonmuscle myosin IIs (*1*). In vertebrate nonmuscle cells, there are three isoforms of myosin II termed myosin IIA, IIB (*1*, *15*−*17*), and the recently identified IIC (*2*, *18*), each

† This work was supported in part by Grant-in-Aid for Scientific Research 14580637 (to M.T.) from the Ministry of Education, Science, Sports, and Culture of Japan.

* To whom correspondence should be addressed: Division of Chemistry, Graduate School of Science, Hokkaido University, Sapporo 060-0810, Japan. Fax: 81-11-706-4924. E-mail: takahash@sci.hokudai.ac.jp.

‡ Division of Chemistry, Graduate School of Science, Hokkaido University.

§ Celestar Lexico-Sciences, Inc.

|| Division of Biological Sciences, Graduate School of Science, Hokkaido University.

⊥ Present address: Shiseido Research Center, Shiseido Co., Ltd., Yokohama, Japan.

@ Present address: Department of Biomolecular Sciences, Graduate School of Life Sciences, Tohoku University, Sendai, Japan.

▽ Present address: Department of Earth and Planetary Science, Graduate School of Science, The University of Tokyo, Tokyo, Japan.

10.1021/bi048807h CCC: $30.25 
Published on Web 12/09/2004

consisting of myosin heavy chain IIA (MHC-IIA), IIB (MHC-IIB), and IIC (MHC-IIC), respectively, and light chains. Differences in subcellular localization between myosin IIA and IIB (*19*−*22*) suggest that these isoforms may assemble differentially and form homogeneous filaments consisting of each isoform in the cells. It was demonstrated that the assembly of myosin IIA and IIB might be regulated in a distinct manner (*23*−*25*).

Although the precise molecular mechanism of filament formation remains to be established even in the case of sarcomeric myosins, it was thought that filament formation proceeded through two steps, that is, the nucleation and elongation steps (*13*, *26*, *27*). Nucleation involves the antiparallel association of two myosin II molecules, and elongation occurs by the addition of monomers to filament ends. A bipolar minifilament consisting of ~30 molecules was formed from purified platelet myosin II (*28*), and the presence of similar minifilaments was observed in fibroblasts (*29*).

Attempts to locate the critical regions for filament formation in myosin II have indicated the importance of the C-terminal region of the rod (*30*−*36*). However, few studies have pursued a more detailed analysis to date. Sohn *et al*. reported that a specific 29-residue region, termed the assembly competence domain (ACD),[1] near the C-terminus of the rod is critical for sarcomeric myosin II assembly (*34*). A region similar to the ACD sequence was found in both smooth muscle and nonmuscle myosin II. Ikebe *et al*. reported that the 28 residues at the C-terminal end of the coiled-coil domain, distinct from the ACD region, are important for the filament formation of both smooth muscle and nonmuscle myosin II (*35*). The studies of the expression of the GFP-fused deletion mutant of myosin II heavy chains in the cultured cell also revealed the importance of the C-terminal region of the rod for the filament formation (*35*, *36*).

In this study, we were able to identify the critical regions for filament formation of vertebrate nonmuscle myosin II by analyzing the solubility properties of a series of truncated recombinant rod fragments of nonmuscle myosin IIB. Further, we constructed a model of an α-helical coiled-coil structure for the myosin IIB rod fragment, and showed that the electrostatic interactions between the three identified regions could be important for the assembly of nonmuscle myosin II molecules.

## MATERIALS AND METHODS

*Plasmid Construction.* Human brain poly(A)$^+$ mRNA was prepared from human brain (whole) total RNA (Clontech) with a BioMag mRNA purification kit (PerSeptive Biosystem). Human brain cDNA was synthesized using a cDNA synthesis kit (Pharmacia) and poly(A)$^+$ mRNA. The DNA encoding the MHC-IIB rod fragment (BRF, 1729−1976) was amplified by PCR using the human brain cDNA library as a template, and primers Bu1 (5′-CGCGGATCCGGATGAGAAGCGGCGTCTGGAAGC-3′) and Bd (5′-CGCGGATCCGCAACTTTACTCTGACTGGGGTGG-3′), with the *Bam*HI site underlined. The amplified DNA was digested with *Bam*HI and subcloned into the *Bam*HI site of the pET15b vector (Novagen) to obtain plasmid pET-BRF, which encodes BRF. The entire nucleotide sequence of the amplified DNA was confirmed by sequencing in both orientations using a sequencer (LI-COR model 4000L DNA sequencer, Aloka). The construct encoding BRFΔN146 (1875−1976) was generated in a similar manner using primer Bu2 (5′-CGCGGATCCGGCCAACGCTCGGATGAAGC-3′) instead of Bu1. The constructs encoding BRFΔC73 (1729−1902) and BRFΔC102 (1729−1874) were generated by PCR using pET-BRF as a template, and primer sets of Bu1 and 5′-CGGGATCCTAGAGTTTACGCCGAGATGCG-3′ and Bu1 and 5′-CGCGGATCCTTACTTCTCCATCTGCTCTTTATAC-3′, respectively. The constructs encoding BRFΔN175 (1904−1976) and BRFΔN35 (1764−1976) were generated by PCR using pET-BRF as a template, and primer sets of 5′-CGCGGATCCGCAGCGGGAACTGGATGATGCCACCG-3′ and Bd and 5′-CGGGATCCGCTACAGGTGGAC-3′ and Bd, respectively. For internal deletion, sense and antisense primers were designed so they would be hybridized to regions of pET-BRF flanking the target site for deletion. For the construct of BRFΔACD28 (deletion from Ala 1875 to Lys 1902), the following primers were used in combination with primers Bu1 and Bd: sense primer, 5′-TAAAGAGCAGATGGAGAAGCTCCAGCGGGAACTGGATGATG-3′; and antisense primer, 5′-CATCCAGTTCCCGCTGGAGCTTCTCCATCTGCTCTTTATAC-3′. For the construct of BRFΔACD56 (deletion from Val 1858 to Ala 1913), the following primers were used in combination with Bu1 and Bd: sense primer, 5′-GCTGAAAGAAATCTTCATGCAGAACGAGGGCCTGAGCCGCGAAG-3′; and antisense primer, 5′-CTTCGCGGCTCAGGCCCTCGTTCTGCATGAAGATTTCTTTCAGC-3′.

*Expression and Purification of Recombinant Proteins.* The *Escherichia coli* BL21(DE3)pLysS cells, transformed with each pET15b construct, were cultured in 250 mL of LB medium supplemented with 50 μM ampicillin and 34 μM chloramphenicol at 37 °C until the $OD_{600}$ reached 0.6. IPTG was then added to a final concentration of 1 mM, and the cells were incubated for a further 6 h. The cells were then harvested by centrifugation at 6000*g* for 5 min at 4 °C. The cell pellet was resuspended in 50 mL of 50 mM Tris-HCl (pH 7.5) and centrifuged at 8000*g* for 5 min at 4 °C. The supernatant was discarded, and the cell pellet was flash-frozen in liquid $N_2$ and stored at −80 °C. The frozen cells were lysed by thawing in a binding buffer [20 mM Tris-HCl (pH 7.9), 0.5 M NaCl, 5 mM imidazole] containing 10 mM $MgCl_2$, 20 μg of DNase I (Sigma), and 0.1 mM PMSF and incubated at room temperature for 20 min. After removal of cell debris by centrifugation at 130000*g* for 20 min, the lysate was loaded onto a $Ni^{2+}$ affinity resin column (His-Bind, Novagen) equilibrated with binding buffer. The column was washed with washing buffer [20 mM Tris-HCl (pH 7.9), 0.5 M NaCl, and 60 mM imidazole]. The recombinant His-tagged proteins were eluted with 20 mM Tris-HCl (pH 7.9), 0.5 M NaCl, and 1 M imidazole. In the case of BRF, the pooled fraction was dialyzed against a low-salt buffer [50 mM sodium phosphate (pH 6.0), 50 mM NaCl, and 2 mM $MgCl_2$] containing 0.1 mM PMSF. The assembled BRF was collected by centrifugation at 12000*g* for 5 min and then dissolved in a high-salt buffer [20 mM Tris-HCl (pH 7.5) and 0.5 M NaCl]. In the case of the other deletion mutants,

[1] Abbreviations: ACD, assembly competence domain; BRF, MHC-IIB rod fragment; ARF, MHC-IIA rod fragment.

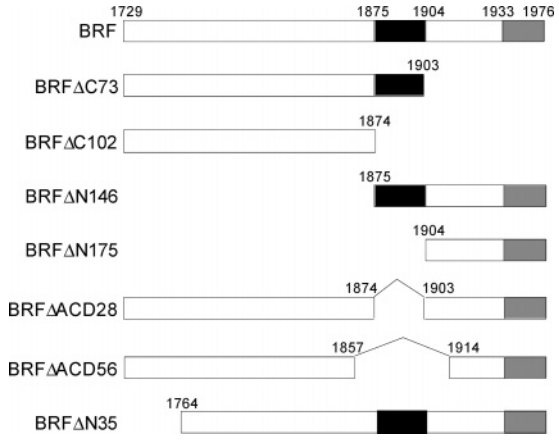


FIGURE 1: Fragments of the C-terminal rod region from human nonmuscle myosin heavy chain IIB expressed in *E. coli*. The size of the human nonmuscle myosin IIB rod fragment, BRF (1729−1976), is approximately one-fifth of the full-length rod. Residue numbers at the regions noted in this study are indicated. Black and gray regions indicate the assembly competence domain (ACD)-like region and the nonhelical tail piece, respectively.

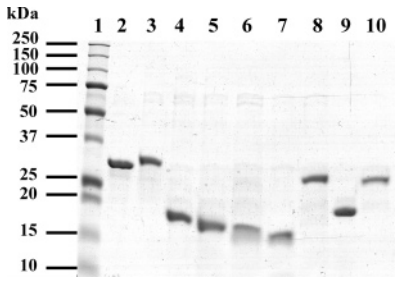


FIGURE 2: SDS−PAGE patterns of the purified rod fragments of nonmuscle myosin II isoforms expressed in *E. coli*: lane 1, Precision Plus Protein Standards (Bio-Rad); lane 2, ARF; lane 3, BRF; lane 4, BRFΔC73; lane 5, BRFΔC102; lane 6, BRFΔN146; lane 7, BRFΔN175; lane 8, BRFΔACD28; lane 9, BRFΔACD56; and lane 10, BRFΔN35.

the pooled fraction was dialyzed against a high-salt buffer containing 0.1 mM PMSF, and then concentrated by ultrafiltration in a VIVASPIN 6 apparatus (Sartrius). The recombinant proteins were digested with 2.5 units of thrombin/mg of protein in 20 mM Tris-HCl (pH 7.5) and 0.25 M NaCl for 16 h at 4 °C, and then dialyzed against a high-salt buffer to remove the His-tag. Each of the resulting fragments contains an extra sequence of Gly-Ser-His-Met-Leu-Glu-Asp-Pro at the N-terminus. The concentrations of the recombinant proteins were measured with the Protein Assay Reagent (Bio-Rad) using BSA as a standard. The profiles of the fragments used in this study are summarized in Figure 1. Figure 2 shows the SDS−PAGE (*37*) pattern of the purified fragments.

*Measurement of the Solubility of Recombinant Fragments.* The solubility of the recombinant myosin II heavy chain rod fragments was examined by ultracentrifugal separation of soluble monomers and precipitation of the assembled fragments after incubation at various salt concentrations. The recombinant rod fragments (0.1 mg/mL) were incubated in 0.05−0.5 M NaCl, 20 mM Tris-HCl (pH 7.5), and 2 mM $MgCl_2$, for 1 h at 4 °C, and then ultracentrifuged at 420000*g* for 20 min at 4 °C. Both the supernatants and the initial reaction mixture before centrifugation were subjected to SDS−PAGE (*37*). The concentrations of monomers in the supernatant and total protein in the initial reaction mixture were determined by a densitometric scan of the CBB-stained gel bands using ATTO Densitograph (ATTO). The solubility was calculated on the basis of the concentration of total protein in the initial reaction mixture being 100%.

*Electron Microscopic Analysis.* Transmission electron microscopy was performed by using a JEOL instrument (JEM-1200EX) at an acceleration voltage of 120 kV. A drop of aggregated rod fragments [0.1 mg/mL fragments, 50 mM NaCl, 20 mM Tris-HCl (pH 7.5), and 2 mM $MgCl_2$] of 10 $\mu$L was put on carbon-coated 200 mesh grids that were rendered hydrophilically by glow discharge at a reduced pressure. After 180 s had passed for adsorption, the grids were stained with 10 $\mu$L of 1% (w/v) uranyl acetate (pH 4.0).

*Construction of the α-Helical Coiled-Coil Structure Model of the Myosin IIB Rod Fragment.* The $C_\alpha$ coordinates of the left-handed coiled-coil structure of the myosin IIB rod fragment were computed on the basis of the parametric equations proposed by Crick (*38*, *39*). The following parameters were used.The radius, the pitch per turn, and the number of residues per turn in α-helix were 2.3 Å, 5.4 Å, and 3.5, respectively; the radius of the coiled coil was 5.2 Å, and the number of heptad repeats in one repeat of the coiled coil was 13. Thus, a pitch of a repeat distance of the computed coiled-coil structure was 140.4 Å. On the basis of the $C_\alpha$ coordinates, a model structure of a coiled-coil region (Asp 1729−Gly 1932) of BRF was constructed using the molecular modeling software SYBYL/COMPOSER (Tripos, Inc.). To maintain the heptad repeat, the initial model was constructed without Lys 1811 that protruded into the heptad structure. The coordinates of the main and side chains of each amino acid except Lys 1811 were added to the constructed $C_\alpha$ coordinates, and then Lys 1811 was inserted into that model. The construction of the coiled-coil model was completed after optimization of the side chain rotamers, addition of the hydrogens, and energy minimization. Construction of the surface structure and the electrostatic potential mapping were performed using SYBYL/MOLCAD (Tripos, Inc.).

## RESULTS

*Short Rod Fragments Contain the Minimum Sequences Critical for Assembly.* Since myosin II molecules assemble into filaments at low ionic strengths and solubilize with an increase in the salt concentration through their electrostatic interaction, quantification of a salt-dependent solubility change in myosin II molecules has been one of the means of estimating the assembly properties of them. The method has also been used to demonstrate the assembly properties of the bacterially expressed rod fragments of various kinds of myosin II heavy chains. In this study, we tried to define the regions critical for the filament assembly of vertebrate nonmuscle myosin II. We expressed various rod fragments of the human nonmuscle myosin heavy chain IIB (Figure 1) and assessed the solubility of these fragments at various NaCl concentrations. We initially chose a MHC-IIB rod fragment (BRF) comprising 248 amino acid residues from the C-terminus (Asp 1729−Glu 1976), and the result was compared with that of peptide ARF (Glu 1722−Glu 1960) derived from a similar region of nonmuscle myosin heavy chain IIA. At

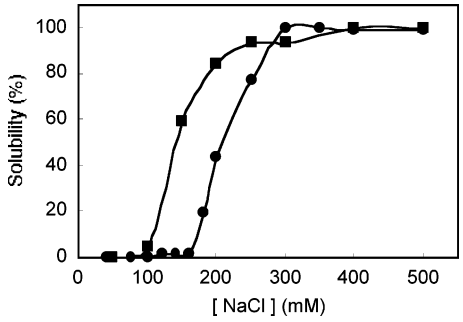


FIGURE 3: Solubility of the rod fragments of nonmuscle myosin II isoforms as a function of NaCl concentration. ARF (■) and BRF (●) were incubated in 20 mM Tris-HCl (pH 7.5) and 2 mM $MgCl_2$ with various concentrations of NaCl. After ultracentrifugation, the concentration of soluble monomers remaining in the supernatant was determined as described in Materials and Methods. The solubility was calculated on the basis of the concentration of total protein in the initial reaction mixture.

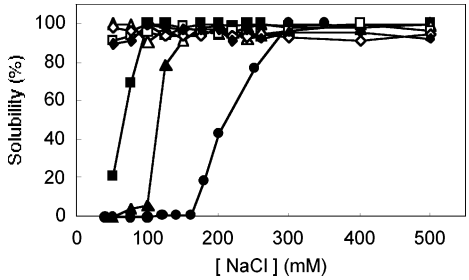


FIGURE 4: Solubility of BRF and its truncated fragments as a function of NaCl concentration. The concentration of soluble monomers was estimated as described in the legend of Figure 2: BRF (●), BRFΔC73 (▲), BRFΔACD28 (■), BRFΔN35 (△), BRFΔACD56 (□), BRFΔC102 (◇), and BRFΔN146 (◆).

the N-terminus, BRF contains one (Asp 1729−Gln 1749) of the regions exhibiting marked amino acid sequence identities among the nonsarcomeric MHCs as pointed out previously (*40*). The nonhelical tail piece and a sequence (Ala 1875−Leu 1903) similar to the ACD of sarcomeric myosins are also contained in BRF.

As shown in Figure 3, the solubility of BRF and ARF decreased with a decrease in the concentration of NaCl. BRF appeared to suffer a decrease in solubility under ionic conditions of around 300 mM NaCl and was almost completely insoluble under physiological salt conditions (150 mM), a concentration at which more than half of the ARF remained soluble. The properties of the solubility of these fragments were similar to the reported properties of much longer rod fragments containing the C-terminal region of each isoform (*23*). This result indicates that BRF and ARF could contain the minimum sequences critical for the assembly of nonmuscle myosin II forms.

*Two Regions Are Required for the Assembly of the IIB Rod Fragment.* To study whether the ACD-like sequence was important for the assembly of BRF, we made six truncated mutants focusing on the region near the ACD-like sequence (Figures 1 and 2). In the creation of the internal deletion mutants, a 28-residue unit was taken into consideration to maintain the periodicity of charged residues. A variety of expressed rod fragments were examined for their solubility at various NaCl concentrations, and the results are shown in Figure 4. BRFΔC73 lacking 73 residues from the C-terminus of BRF but retaining the ACD-like sequence was soluble at a concentration of NaCl of <0.15 M, indicating its weaker ability to assemble compared to the ability of BRF. BRFΔC102 with a further C-terminal deletion, lacking the ACD-like sequence as well, was completely soluble even at 0.05 M NaCl. These results indicate that the ACD-like sequence is necessary but not sufficient for the assembly of BRF, and some residues on the C-terminal side of the ACD-like sequence are also required. Since BRFΔN146 consisting of a region from the ACD-like sequence to the C-terminal end was completely soluble even at lower NaCl concentrations, some of the N-terminal region of the ACD-like sequence is also required for assembly. BRFΔN175, lacking the ACD-like sequence region of BRFΔN146, was also completely soluble under all conditions that were tested (data not shown). BRFΔACD28 lacking 28 residues of the ACD-like sequence of BRF was barely insoluble at the concentration of NaCl lower than 0.1 M, indicating its ability to assemble is weaker than that of BRFΔC73. BRFΔACD56 lacking a further 17 and 10 residues of the N-terminal and C-terminal sides of ACD-like sequence, respectively, from BRFΔACD28 failed to precipitate under any conditions that were tested. These results taken together suggest (1) there is a region necessary for the assembly of myosin IIB within the 39 residues (Ala 1875−Ala 1913) which includes the ACD-like sequence and (2) there is another essential region for assembly somewhere within the N-terminal region of BRF that can interact with the region (Ala 1875−Ala 1913). The results showing both BRFΔC102 and BRFΔN146, each consisting of the N-terminal side of Lys 1874 and the C-terminal side of Ala 1875, respectively, failed to precipitate under any conditions that were tested strongly support this assumption.

The amino acid sequence of the 39-residue region (Ala 1875−Ala 1913) shows a characteristic arrangement of charged residues. Positive and negative clusters are alternatively aligned twice from the N-terminus of this region (Figure 5). We have searched for a region accommodating and interacting with the characteristic arrangement of the 39-residue region within the N-terminal side of BRF on the basis of the primary structure. An N-terminal region of BRF consisting of 35 residues (Asp 1729−Thr 1763) was suggested as a candidate. To check this possibility, we constructed a deletion mutant (BRFΔN35) of this region and examined its solubility (Figure 4). BRFΔN35 could not be precipitated at any salt condition, which supports the idea that the N-terminal 35-residue region (Asp 1729−Thr 1763) could be a region interacting with the 39 residues (Ala 1875−Ala 1913). The regions were termed nACD1 and nACD2, respectively.

Next, we attempted to assess the critical monomer concentration for assembly of the three fragments, BRF, BRFΔC73, and BRFΔACD28. Since BRF was precipitated even at concentrations as low as 10 $\mu$g/mL at 125 mM NaCl, we could not determine the exact critical concentration by this method (Figure 6). In contrast, almost all of the BRFΔC73 and BRFΔACD28 added to the reaction mixtures was recovered in the supernatant at 125 mM NaCl. Even at the increased concentration of 500 $\mu$g/mL, both fragments were not precipitated under this ionic condition (data not shown). At 50 mM NaCl, the critical concentrations of BRFΔC73 and BRFΔACD28 were estimated to be ∼10 and ∼20 $\mu$g/mL, respectively. These results are consistent with

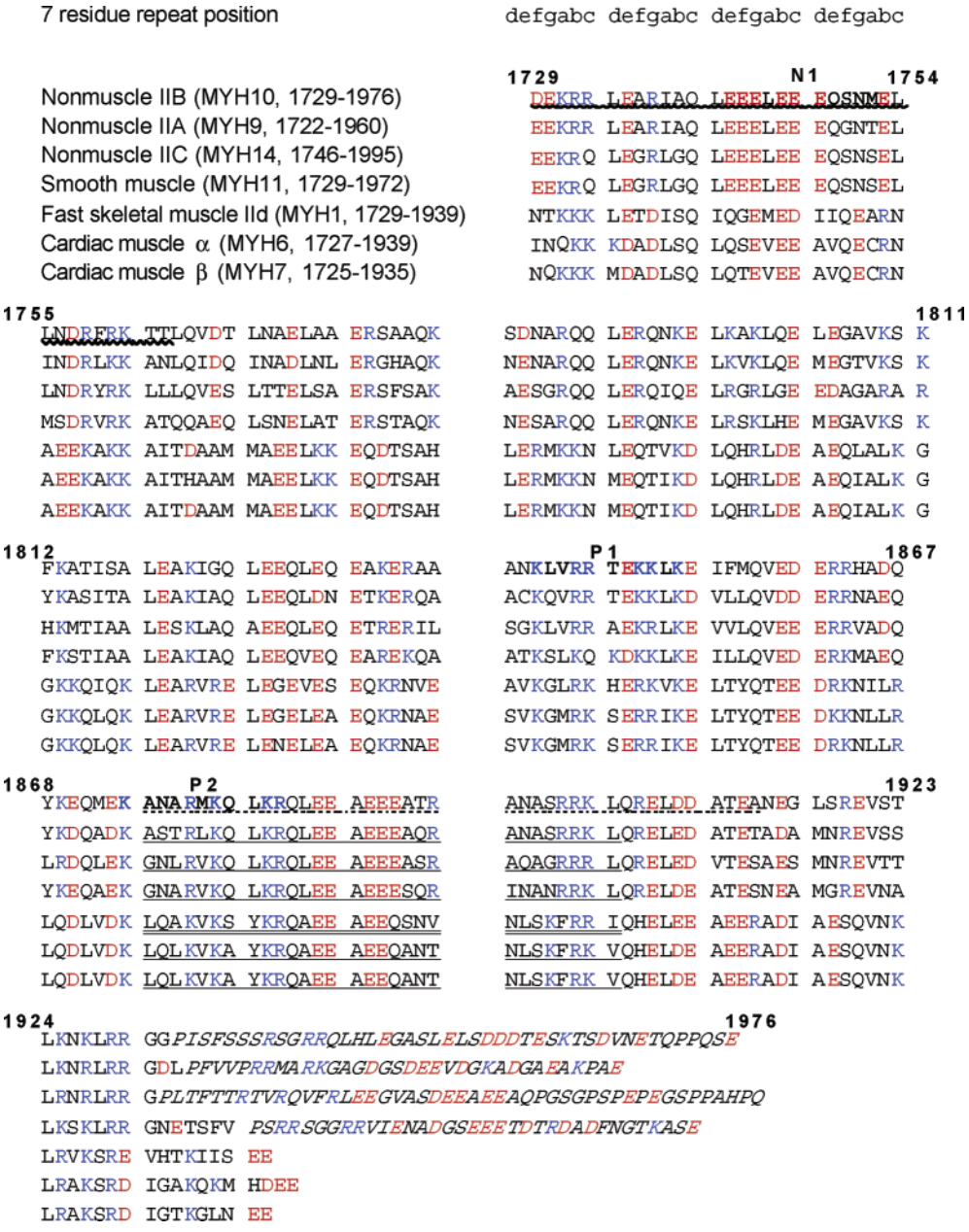


FIGURE 5: Alignment of the sequences of human myosin II heavy chains in regions homologous to BRF. Heptad repeat positions are indicated above the sequences. Double and single underlines indicate the ACD sequence and ACD-like sequence of various human myosins, respectively (*34*). Wave and dotted lines indicate nACD1 and nACD2 identified in this study, respectively. Bold characters indicate the negative charge cluster (N1) and the two positive charge clusters (P1 and P2). Italic characters indicate nonhelical tail pieces. Residue numbers for MHC-IIB are given. Sequence data were obtained by GenBank from the following sources: MYH10 (*41*), MYH9 (*42*), MYH14 (*2*), MYH11 (*43*), MYH1 (*44*), MYH6 (*45*), and MYH7 (*46*).

the assembly properties of these fragments evaluated from the solubility at various NaCl concentrations.

The structures of BRF, BRFΔC73, and BRFΔACD28 were observed by electron microscopy at 50 mM NaCl. The BRF was shown to be a filamentous structure (Figure 7). On the other hand, BRFΔC73 and BRFΔACD28 experienced disordered aggregation. These results suggest that only BRF would be capable of carrying out ordered assembly like a native filament.

*Construction of an α-Helical Coiled-Coil Model of the IIB Rod Fragment.* There is no question that the myosin II tail forms an α-helical coiled-coil structure consisting of two heavy chains because of the highly distinctive feature of its primary structure and also of its electron microscopic image.

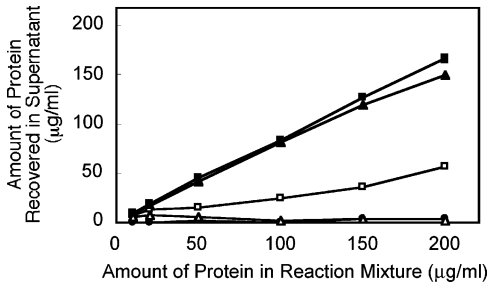


FIGURE 6: Critical monomer concentration for assembly of BRF and its truncated fragments. The critical concentrations for BRF (circles), BRFΔC73 (triangles), and BRFΔACD28 (squares) were estimated under the following conditions: 20 mM Tris-HCl (pH 7.5) and 2 mM $MgCl_2$ with 125 mM NaCl (filled symbols) or with 50 mM NaCl (empty symbols).

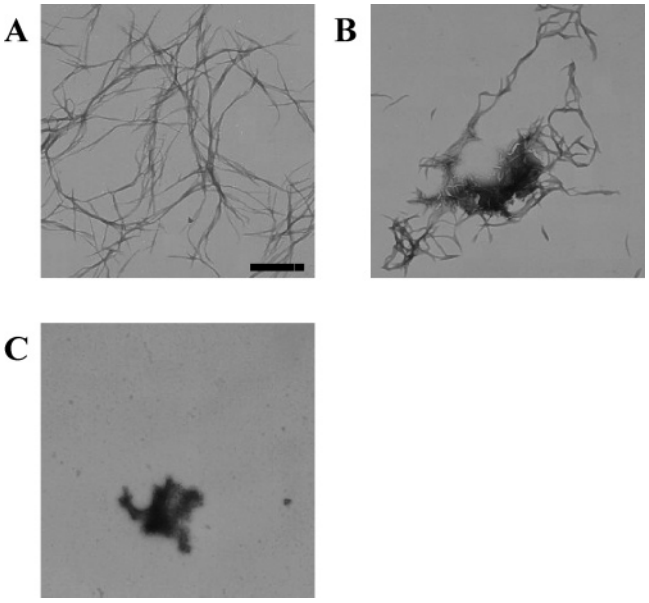


FIGURE 7: Electron micrographs of rod fragments under low-salt conditions. The structure of BRF and its truncated fragments was observed by electron microscopy at 50 mM NaCl, 20 mM Tris-HCl (pH 7.5), and 2 mM $MgCl_2$: (A) BRF, (B) BRFΔC73, and (C) BRFΔACD28. The bar represents 1.0 $\mu$m.

BRF has a typical amino acid sequence for the α-helical coiled-coil structure except for the nonhelical tail pieces (Figure 5). A quaternary structure model of a coiled-coil region (Asp 1729−Gly 1932) of BRF was constructed on the basis of Crick's coiled-coil model (Figure 7). Lys 1811 is a skip residue interrupting the regular heptad repeat; therefore, a basic model with the exception of this residue was first constructed, and then this residue was inserted into the model. Mapping of electrostatic potential on the surface of the constructed model revealed a remarkable negative charge cluster (Glu 1742−Glu 1753, termed N1) and a positive charge cluster (Lys 1874−Arg 1884, termed P2) present within nACD1 and nACD2, respectively. Moreover, another positive charge cluster (Lys 1842−Lys 1852, termed P1) was present in the N-terminal side of nACD2. These three regions, two of which are involved in nACD1 and nACD2, may be important for electrostatic interactions between the fragments for their assembly.

## DISCUSSION

In this report, we described the role of two regions in the C-terminal region of nonmuscle MHC-IIB that are required for filament assembly. It was shown that fragments lacking either nACD1 or nACD2 were soluble at any NaCl concentration. We constructed an α-helical coiled-coil structure model of the MHC-IIB rod fragment, which indicated the existence of negative charge cluster N1 and two positive charge clusters, P1 and P2 (Figure 8). We hypothesize that the electrostatic interaction among these charge clusters would be important for the nucleation step of filament formation and also for elongation.

We considered the mode of the interaction between the two rod fragments on the basis of the electrostatic potential map on the molecular surfaces of the constructed model (Figure 9). Figure 9A shows the best match mode for antiparallel interaction, which is formed mainly by the electrostatic interactions between N1 and P2, and additionally between the C-terminal region from nACD1 and P1 of each fragment. The length of the antiparallel overlap between myosin II molecules has not been established yet. Kendrick-Jones *et al*. first indicated that smooth muscle myosin rods formed a 43 nm antiparallel overlap when they were precipitated with divalent cations (*47*). Nonmuscle myosin II rods from brain formed an equivalent assembly structure (*48*). 10S monomers of smooth muscle myosin formed an antiparallel folded dimer with an approximately 45 nm overlap at very low ionic strengths (*49*, *50*) as well as 6S monomers (*51*). Interestingly, our antiparallel model exhibits a molecular overlap similar to the reported length (Figure 9A) if we add the nonhelical tail pieces to each C-terminal end, although the exact length of the nonhelical tail piece has not been determined yet. On the other hand, Figure 9B shows the best mode for parallel interaction of the constructed model, which is formed mainly by the electrostatic interaction between N1 and P1 of each fragment, giving an ∼14 nm stagger between two fragments. This length is close to that of widely observed axial stagger between neighboring molecules in the filament of sarcomeric myosin (*52*) as well as nonsarcomeric myosins (*53*). The positions of the charged residues in both nACD1 and nACD2 are compatible with a common 28-residue repeating unit involved in the interaction between neighboring molecules. Besides the agreement with the periodicities in sequence, the extent of negative and positive charges at N1 and P1 or P2, respectively, was prominent in the constructed model. The expected strong interactions among these clusters can be supported further by the charge distribution in the vicinity which is favorable for the stabilization of filaments. The antiparallel interaction could be much more stable than the parallel one, because the former contains two strong interaction sites consisting of N1 and P2 while the latter contains only one site consisting of N1 and P1 between two molecules (Figure 9). It is noteworthy that both the antiparallel and parallel models presented here showed good fits between two fragments in shape as well as in electrostatic interaction.

We demonstrate here that the corresponding region of the ACD proposed in sarcomeric myosin with a few residues at its C-terminal sides, nACD2, would be important for molecular assembly even in nonsarcomeric-type myosin II by estimation of the solubility properties of rod fragments. It is noted that the region of nACD2 considerably overlaps with the extended ACD proposed by Cohen and Parry (*54*). Further, we found the presence of the region (nACD1) interacting with the ACD or extended ACD in nonmuscle myosin II, which was predicted previously in sarcomeric myosin (*34*, *54*). The sequence of nACD1 is specific for nonsarcomeric-type myosin II molecules, although that of nACD2 is conserved among the corresponding regions of myosin II molecules (Figure 5). The remarkable property of the nACD1 is the paucity of positive charge residues at the central portion. There is a long stretch with eight negative and no positive charge residues within 20 amino acids (Ile 1738−Asp 1757), possibly leading to a negative charge cluster, N1, in this region. A long stretch without positive charge (18 or 19 amino acids) also exists within a corresponding region of nACD1 in sarcomeric-type myosin II forms, though there are not so many negative charge residues compared to the number in nonsarcomeric-type myosin II

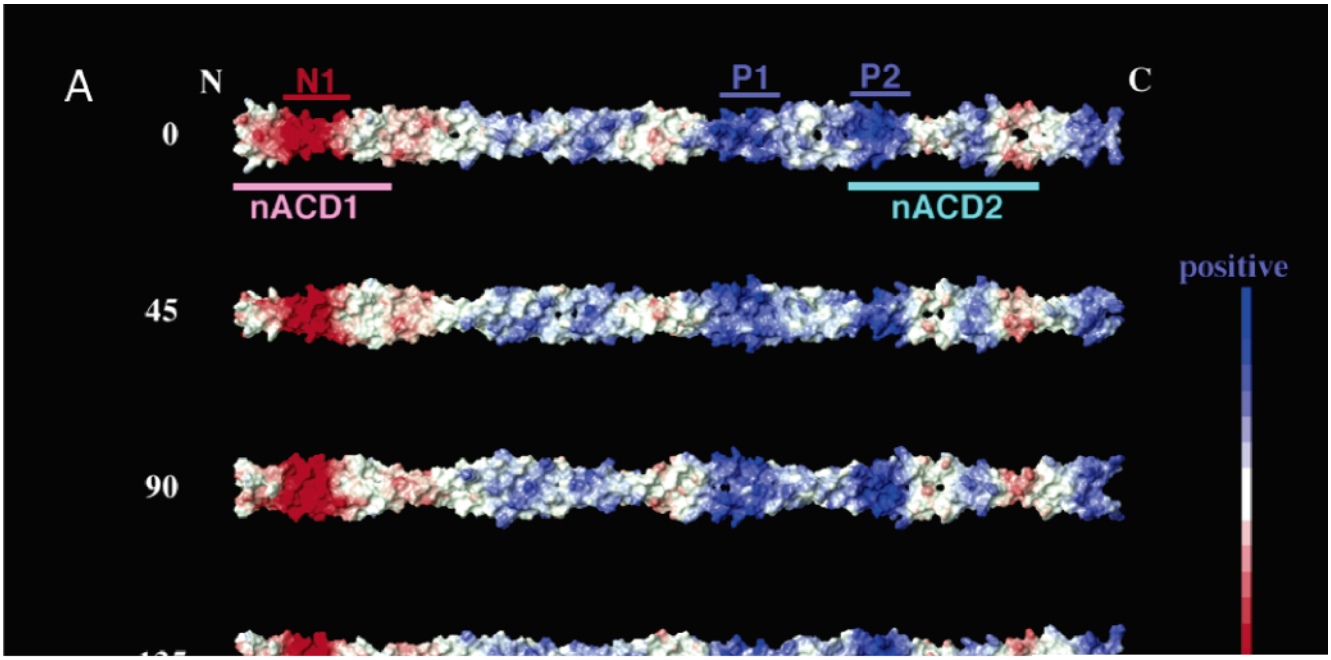


FIGURE 8: Structural model of the α-helical coiled-coil portion (Asp 1729−Gly 1932) of BRF. (A) Electrostatic surface potential. The intensity of surface colors red and blue represents the extent of electrostatic potential, negative and positive, respectively. The regions nACD1 and nACD2 are indicated by colored underlines. The remarkable negative charge cluster (N1) and positive charge clusters (P1 and P2) are also indicated. Shown here are four views obtained by rotating the molecules counterclockwise viewed from N-terminal side along a rod axis (0°, 45°, 90°, and 135° as indicated). (B) N1, P1, and P2 regions of BRF. All protein atoms are shown as space-filling models. Each myosin heavy chain is shown with different colors, cyan and yellow. In these images, nitrogen atoms (as a positive charge indicator) and oxygen atoms (as a negative charge indicator) are colored blue and red, respectively. Enlarged views of N1, P1, and P2 regions were shown with their amino acid sequences.

forms (Figure 5). Actually, the fragment of skeletal muscle myosin II equivalent to BRF was able to assemble, but the one lacking this region was not (*34*). Although we need further information about whether this region has properties similar to those of nACD1, the nucleation step of myosin II molecules might be basically similar in the sarcomeric and nonsarcomeric types.

The truncated fragments (BRFΔC73 and BRFΔACD28) that failed to assemble under physiological ionic conditions might associate in ways different from those of the regular modes indicated in Figure 9 under very low-salt conditions. Actually, electron micrographic observation revealed that BRFΔC73 and BRFΔACD28 experienced disordered aggregation (Figure 7). The distribution of electrostatic potential

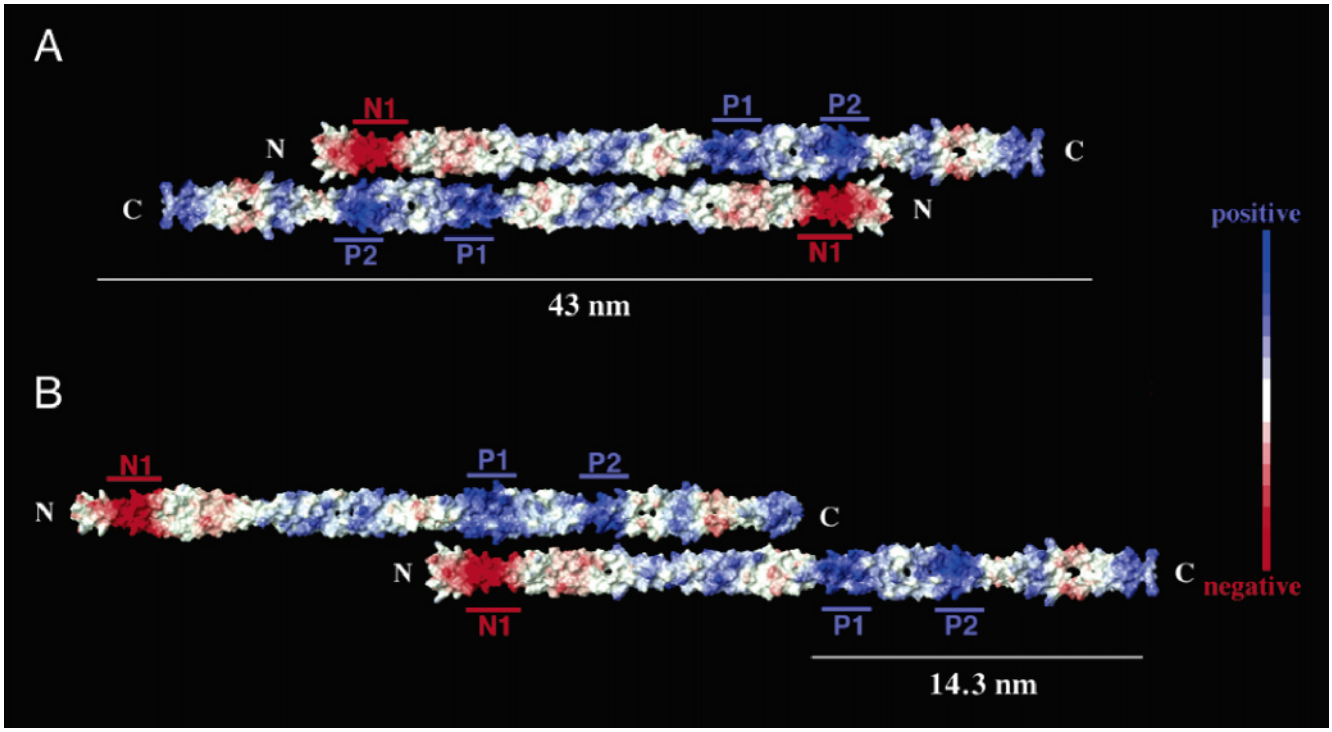


FIGURE 9: Molecular packing models of BRF. (A) Antiparallel model. Interaction between N1 and P2 of each fragment is major in this mode. An underline indicates the expected overlap length (43 nm) of each molecule including the nonhelical tail piece. Note that each molecule is oriented with the same surface (the view of 0° in Figure 6A) facing the viewer. (B) Parallel model. Interaction between N1 and P2 of each fragment is major in this mode. An underline indicates the stagger length (14.3 nm) between each molecule. Note that the top molecule is oriented with a view of a 40° rotation relative to the bottom one (the view of 0° in Figure 6A).

on the surface of these fragments changed slightly from the original one (data not shown), causing a different mode of association. The truncated fragments (BRFΔC102 and BRFΔACD56) failed to precipitate even at very low ionic strengths. These fragments might be able to perform only parallel interactions. The nucleation step caused by antiparallel interactions would be indispensable for a filament formation so that both BRFΔC102 and BRFΔACD56 might fail to assemble.

It has been demonstrated that the C-terminal region from nACD2 was also important for filament formation (*23*−*25*, *33*, *35*, *55*, *56*). The 28 residues from the C-terminal end of the coiled-coil domain of smooth muscle myosin and nonmuscle myosin IIA were shown to be critical for filament formation (*35*). It was shown that the antibodies recognizing the 28 residues from the C-terminal end of the coiled-coil domain of smooth muscle myosin inhibited filament formation (*35*). We suppose that the antibody against this region may sterically prevent the interaction between nACD1 and nACD2 because of its large size, like the inhibitory effect of mts1 (a member of the S100 family of $Ca^{2+}$-binding proteins) on the assembly of nonmuscle myosin IIA *in vitro* (*24*, *25*). This region would have a regulatory role for filament formation when nACD1 and nACD2 interact with each other between myosin II molecules. The nonhelical tail piece might also influence the interaction between nACD1 and nACD2. Deletion of the nonhelical tail piece of myosin IIA resulted in an increase in the critical concentration for assembly (*33*). Assembly of myosin IIB was significantly inhibited by the phosphoryltaion of its nonhelical tail piece (*23*, *24*). The alternatively spliced isoforms of smooth muscle myosin heavy chains that differ at their nonhelical tail pieces exhibited different properties during filament assembly (*55*, *56*). The filament assembly of *Dictyostelium* myosin II is regulated by phosphorylation at three Thr residues in the tail region (*10*−*12*). Besides the regulation by phosphorylation of the regulatory light chains, vertebrate nonmuscle myosin II molecules might have a regulatory mechanism for assembly in the tail region analogous to that of *Dictyostelium* myosin II. The C-terminal region of nACD2 could take part in such a regulatory mechanism by affecting the interaction between nACD1 and nACD2, which is required for the nucleation step of filament formation.

The solubility properties of truncated rod fragments and the results of molecular modeling presented in this paper indicated that the extended ACD-like region (nACD2) is important for the filament formation of nonmuscle myosin II. Moreover, we identified nACD1 as the target site of nACD2. We propose that the antiparallel interaction between N1 and P2 located within these regions is essential for the nucleation step of nonmuscle myosin II assembly and the parallel interaction between N1 and P1 is important for the elongation step. Further studies will reveal how myosin II molecules form filaments through the interaction of these regions.

## ACKNOWLEDGMENT

We thank Dr. R. S. Adelstein (National Heart, Lung, and Blood Institute, National Institutes of Health, Bethesda, MD) for his helpful discussion and critical reading of the manuscript. We also thank Dr. Y. Osada, Dr. J. P. Gong, and Mr. K. Shikinaka (Hokkaido University, Sapporo, Japan) for critical discussion.

## REFERENCES

1. Sellers, J. R. (1999) *Myosins*, 2nd ed., Oxford University Press, Oxford, U.K.

2. Berg, J. S., Powell, B. C., and Cheney, R. E. (2001) A millennial myosin census, *Mol. Biol. Cell 12*, 780−794.
3. Parry, D. A. D. (1981) Structure of rabbit skeletal myosin: Analysis of the amino acid sequences of two fragments from the rod region, *J. Mol. Biol. 153*, 459−464.
4. McLachlan, A. D., and Karn, J. (1982) Periodic charge distribution in the myosin rod amino acid sequence match cross-bridge spacings in muscle, *Nature 299*, 226−231.
5. Trybus, K. M. (1991) Assembly of cytoplasmic and smooth muscle myosins, *Curr. Opin. Cell Biol. 3*, 105−111.
6. Somlyo, A. V., Butler, T. M., Bond, M., and Somlyo, A. P. (1981) Myosin filaments have non-phosphorylated light chains in relaxed smooth muscle, *Nature 294*, 567−569.
7. Xu, J.-Q., Harder, B. A., Uman, P., and Craig, R. (1996) Myosin filament structure in vertebrate smooth muscle, *J. Cell Biol. 134*, 53−66.
8. Egelhoff, T. T., Lee, R. J., and Spudich, J. A. (1993) *Dictyostelium* myosin heavy chain phosphorylation sites regulate myosin filament assembly and localization in vivo, *Cell 75*, 363−371.
9. Yumura, S. (2001) Myosin II dynamics and cortical flow during contractile ring formation in *Dictyostelium* cells, *J. Cell Biol. 154*, 137−146.
10. O'Halloran, T. J., Ravid, S., and Spudich, J. A. (1990) Expression of *Dictyostelium* myosin tail segments in *Escherichia coli*: Domains required for assembly and phosphorylation, *J. Cell Biol. 110*, 63−70.
11. Shoffner, J. D., and De Lozanne, A. (1996) Sequences in the myosin II tail required for self-association, *Biochem. Biophys. Res. Commun. 218*, 860−864.
12. Liang, W., Warrick, H. M., and Spudich, J. A. (1999) A structural model for phosphorylation control of *Dictyostelium* myosin II thick filament assembly, *J. Cell Biol. 147*, 1039−1047.
13. Sinard, J. H., Stafford, W. F., and Pollard, T. D. (1989) The mechanism of assembly of *Acanthamoeba* myosin-II minifilaments: Minifilaments assemble by three successive dimerization steps, *J. Cell Biol. 109*, 1537−1547.
14. Sinard, J. H., Rimm, D. L., and Pollard, T. D. (1990) Identification of functional regions on the tail of *Acanthamoeba* myosin-II using recombinant fusion proteins. II. Assembly properties of tails with $NH_2$- and COOH-terminal deletions, *J. Cell Biol. 111*, 2417−2426.
15. Katsuragawa, Y., Yanagisawa, M., Inoue, A., and Masaki, T. (1989) Two distinct nonmuscle myosin-heavy-chain mRNAs are differentially expressed in various chicken tissues. Identification of a novel gene family of vertebrate non-sarcomeric myosin heavy chains, *Eur. J. Biochem. 184*, 611−616.
16. Kawamoto, S., and Adelstein, R. S. (1991) Chicken nonmuscle myosin heavy chains: Differential expression of two mRNAs and evidence for two different polypeptides, *J. Cell Biol. 112*, 915−924.
17. Bresnick, A. R. (1999) Molecular mechanisms of nonmuscle myosin-II regulation, *Curr. Opin. Cell Biol. 11*, 26−33.
18. Golomb, E., Ma, X., Jana, S. S., Preston, Y. A., Kawamoto, S., Shoham, N. G., Goldin, E., Conti, M. A., Sellers, J. R., and Adelstein, R. S. (2004) Identification and Characterization of Nonmuscle Myosin II-C, a New Member of the Myosin II Family, *J. Biol. Chem. 279*, 2800−2808.
19. Maupin, P., Phillips, C. L., Adelstein, R. S., and Pollard, T. D. (1994) Differential localization of myosin-II isozymes in human cultured cells and blood cells, *J. Cell Sci. 107*, 3077−3090.
20. Kelley, C. A., Sellers, J. R., Gard, D. L., Bui, D., Adelstein, R. S., and Baines, I. C. (1996) *Xenopus* nonmuscle myosin heavy chain isoforms have different subcellular localization and enzymatic activities, *J. Cell Biol. 134*, 675−687.
21. Saitoh, T., Takemura, S., Ueda, K., Hosoya, H., Nagayama, M., Haga, H., Kawabata, K., Yamagishi, A., and Takahashi, M. (2001) Differential localization of non-muscle myosin II isoforms and phosphorylated regulatory light chains in human MRC-5 fibroblasts, *FEBS Lett. 509*, 365−369.
22. Kolega, J. (2003) Asymmetric distribution of myosin IIB in migrating endothelial cells is regulated by a rho-dependent kinase and contributes to tail retraction, *Mol. Biol. Cell 14*, 4745−4757.
23. Murakami, N., Singh, S. S., Chauhan, V. P. S., and Elzinga, M. (1995) Phospholipid binding, phosphorylation by protein kinase C, and filament assembly of the COOH terminal heavy chain fragments of nonmuscle myosin II isoforms MIIA and MIIB, *Biochemistry 34*, 16046−16055.
24. Murakami, N., Kotula, L., and Hwang, Y. W. (2000) Two distinct mechanisms for regulation of nonmuscle myosin assembly via the heavy chain: Phosphorylation for MIIB and Mts 1 binding for MIIA, *Biochemistry 39*, 11441−11451.
25. Li, Z. H., Spektor, A., Varlamova, O., and Bresnick, A. R. (2003) Mts 1 regulates the assembly of nonmuscle myosin-IIA, *Biochemistry 42*, 14258−14266.
26. Huxley, H. E. (1963) Electron microscope studies on the structure of natural and synthetic protein filaments from striated muscle, *J. Mol. Biol. 7*, 281−308.
27. Cross, R. A., Geeves, M. A., and Kendrick-Jones, J. (1991) A nucleation−elongation mechanism for the self-assembly of side polar sheets of smooth muscle myosin, *EMBO J. 10*, 747−756.
28. Niederman, R., and Pollard, T. D. (1975) Human platelet myosin. II. In vitro assembly and structure of myosin filaments, *J. Cell Biol. 67*, 72−92.
29. Verkhovsky, A. B., and Borisy, G. G. (1993) Non-sarcomeric mode of myosin II organization in the fibroblast lamellum, *J. Cell Biol. 123*, 637−652.
30. Nyitray, L., Mocz, G., Szilagyi, L., Balint, M., Lu, R. C., Wong, A., and Gergely, J. (1983) The proteolytic substructure of light meromyosin. Localization of a region responsible for the low ionic strength insolubility of myosin, *J. Biol. Chem. 258*, 13213−13220.
31. Cross, R. A., and Vandekerckhove, J. (1986) Solubility-determining domain of smooth muscle myosin rod, *FEBS Lett. 200*, 355−360.
32. Atkinson, S. J., and Stewart, M. (1991) Expression in *Escherichia coli* of fragments of the coiled-coil rod domain of rabbit myosin: Influence of different regions of the molecule on aggregation and paracrystal formation, *J. Cell Sci. 99*, 823−836.
33. Hodge, T. P., Cross, R., and Kendrick-Jones J. (1992) Role of the COOH-terminal nonhelical tailpiece in the assembly of a vertebrate nonmuscle myosin rod, *J. Cell Biol. 118*, 1085−1095.
34. Sohn, R. L., Vikstrom, K. L., Strauss, M., Cohen, C., Szent-Györgyi, A. G., and Leinwand, L. A. (1997) A 29 residue region of the sarcomeric myosin rod is necessary for filament formation, *J. Mol. Biol. 266*, 317−330.
35. Ikebe, M., Komatsu, S., Woodhead, J. L., Mabuchi, K., Ikebe, R., Saito, J., Craig, R., and Higashihara, M. (2001) The tip of the coiled-coil rod determines the filament formation of smooth muscle and nonmuscle myosin, *J. Biol. Chem. 276*, 30293−30300.
36. Wei, Q., and Adelstein, R. S. (2000) Conditional expression of a truncated fragment of nonmuscle myosin II-A alters cell shape but not cytokinesis in HeLa cells, *Mol. Biol. Cell 11*, 3617−3627.
37. Porzio, M. A., and Pearson, A. M. (1977) Improved resolution of myofibrillar proteins with sodium dodecyl sulfate-polyacrylamide gel electrophoresis, *Biochim. Biophys. Acta 490*, 27−34.
38. Crick, F. H. C. (1953) The Fourier transform of a coiled-coil, *Acta Crystallogr. 6*, 685−689.
39. Crick, F. H. C. (1953) The packing of α-helices: Simple coiled-coils, *Acta Crystallogr. 6*, 689−697.
40. Takahashi, M., Kawamoto, S., and Adelstein, R. S. (1992) Evidence for inserted sequences in the head region of nonmuscle myosin specific to the nervous system: Cloning of the cDNA encoding the myosin heavy chain-B isoforms of vertebrate nonmuscle myosin, *J. Biol. Chem. 267*, 17864−17871.
41. Phillips, C. L., Yamakawa, K., and Adelstein, R. S. (1995) Cloning of the cDNA encoding human nonmuscle myosin heavy chain-B and analysis of human tissues with isoform-specific antibodies, *J. Muscle Res. Cell Motil. 16*, 379−389.
42. Saez, C. G., Myers, J. C., Shows, T. B., and Leinwand, L. A. (1990) Human nonmuscle myosin heavy chain mRNA: Generation of diversity through alternative polyadenylylation, *Proc. Natl. Acad. Sci. U.S.A. 87*, 1164−1168.
43. Matsuoka, R., Yoshida, M. C., Furutani, Y., Imamura, S., Kanda, N., Yanagisawa, M., Masaki, T., and Takao, A. (1993) Human smooth muscle myosin heavy chain gene mapped to chromosomal region 16p12, *Am. J. Med. Genet. 46*, 61−67.
44. Saez, L., and Leinwand, L. A. (1986) Characterization of diverse forms of myosin heavy chain expressed in adult human skeletal muscle, *Nucleic Acids Res. 14*, 2951−2969.
45. Matsuoka, R., Beisel, K. W., Furutani, M., Arai, S., and Takao, A. (1991) Complete sequence of human cardiac α-myosin heavy chain gene and amino acid comparison to other myosins based

on structural and functional differences, *Am. J. Med. Genet. 41*, 537−547.
46. Jandreski, M. A., and Liew, C. C. (1987) Construction of a human ventricular cDNA library and characterization of a $\beta$-myosin heavy chain cDNA clone, *Hum. Genet. 76*, 47−53.
47. Kendrick-Jones, J., Szent-Györgyi, A. G., and Cohen, C. (1971) Segments from vertebrate smooth muscle myosin rods, *J. Mol. Biol. 59*, 527−529.
48. Barylko, B., Dobrowolki, Z., and Karasinski, J. (1989) The assembly of the rod portion of brain myosin, *Eur. J. Cell Biol. 48*, 264−270.
49. Onishi, H., and Wakabayashi, T. (1984) Electron microscopic studies on myosin molecules form chicken gizzard muscle III, *J. Biochem. 95*, 903−905.
50. Trybus, K. M., and Lowey, S. (1984) Conformational states of smooth muscle myosin, *J. Biol. Chem. 259*, 8564−8571.
51. Trybus, K. M., and Lowey, S. (1987) Assembly of smooth muscle myosin minifilaments: Effects of phosphorylation and nucleotide binding, *J. Cell Biol. 105*, 3007−3019.
52. Huxley, H. E., and Brown, W. (1967) The low-angle X-ray diagram of vertebrate striated muscle and its behavior during contraction and rigor, *J. Mol. Biol. 30*, 383−434.
53. Small, J. V., and Squire, J. M. (1972) Structural basis of contraction in vertebrate smooth muscle, *J. Mol. Biol. 67*, 117−149.
54. Cohen, C., and Parry, D. A. D. (1998) A conserved C-terminal assembly region in paramyosin and myosin rods, *J. Struct. Biol. 122*, 180−187.
55. Quevillon-Chéruel, S., Foucault, G., Desmadril, M., Lompré, A. M., and Béchet, J. J. (1999) Role of the C-terminal extremities of the smooth muscle myosin heavy chains: Implication for assembly properties, *FEBS Lett. 454*, 303−306.
56. Rovner, A. S., Fagnant, P. M., Lowey, S., and Trybus, K. M. (2002) The carboxyl-terminal isoforms of smooth muscle myosin heavy chain determine thick filament assembly properties, *J. Cell Biol. 156*, 113−123.

BI048807H